Mineral Res. Expl. Bull., 140, 19-34, 2010

INVESTIGATIONS OF ALTERATION ZONES BASED ON FLUID INCLUSION MICROTHERMOMETRY AT SUNGUN PORPHYRY COPPER DEPOSIT, NW IRAN

Omid ASGHARI* and Ardeshir HEZARKHANI**

ABSTRACT.- The Sungun porphyry copper deposit is located in East Azerbaijan, NW of Iran. The porphyries occur as stocks and dikes ranging in composition from quartz monzodiorite to quartz monzonite. Four types of hypogene alteration are developed; potassic, phyllic, propylitic and argillic. Three types of fluid inclusions are typically observed at Sungun; (1) vapor-rich, (2) liquid-rich and (3) multi-phase. Halite is the principal solid phase in the latter. The primary multiphase inclusions within the quartz crystals were chosen for micro-thermometric analyses and considered to calculate the geological pressure and hydrothermal fluid density. In potassic zone, the average of homogenization temperature is 413.6 °C while in phyllic alteration, 375.9 °C. As expected in potassic alteration, the temperature of hydrothermal solutions is higher than that in phyllic zone. The salinity of the hydrothermal fluids has a high coherency with homogenization temperature, so the average of salinity in potassic samples is 46.3 (wt% NaCl) which is higher than phyllic samples. Based on the location of potassic alteration, as expected, the lithostatic pressure is much more than the phyllic one. Finally, the average density of hydrothermal fluids in the potassically altered samples is 1.124 (gr/cm^3) which is higher than the ones in phyllic zone (1.083 gr/cm^3).

Key words: Fluid Inclusion, Porphyry copper deposit, Potassic alteration, Phyllic alteration, Microthermometry, Sungun, İran.

INTRODUCTION

Porphyry Copper deposits are generated where magmatic - hydrothermal fluids are expelled from a crystallizing magma (Burnham, 1979; Ulrich et al. 2001). Cooling, depressurization, and reaction between the fluids and the wall rocks cause metals to precipitate in and around the fractures, forming veins with alteration envelopes. Alteration assemblages and associated mineralization in porphyry ore deposits develop from huge hydrothermal systems dominated by magmatic and meteoric fluids (Sillitoe 1997; Hedenquist and Richards 1998). These systems develop in and adjacent to subvolcanic porphyritic intrusions that are apophyses of deeper-seated magma bodies (Dilles and Einaudi 1992; Sillitoe and Hedenquist 2003; Heinrich et al. 2003). Fluid inclusion analyses indicate that, the inclusions which are trapped in porphyry Cu deposits, typically include halite-saturated brines and low-salinity vapor inclusions (Nash, 1976; Roedder, 1984; Beane and Bodnar, 1995; Tosdal and Richards 2001; Heinrich, 2005). The formation of brine and vapor are inferred to result from a miscibility gap in the NaCl-H_2O system that coincides with the pressure (< 2200 bars) and temperature (300 to 600°C) where most porphyry Cu deposits form (Sourirajan and Kennedy, 1962; Urusova, 1975; Roedder and Bodnar 1980; Beane and Bodnar, 1995; Kehayov et al. 2003).

Fluid inclusion studies in porphyry copper deposits (PCDs) have proven to be an important tool to constrain the physico-chemical conditions of the hydrothermal fluids responsible for vast and pervasive alteration and mineralization processes. These fluid inclusion studies have shown many common features in such deposits throughout the world (Nash, 1976; Chivas and Wilkins, 1977; Beane and Titley, 1981; Roedder, 1984; Quan et al., 1987; Beane and Bodnar, 1995; Ulrich et al. 2001; Redmond et al. 2004).

* Department of Mining Engineering, University of Kashan, Kashan, I.R.Iran (E-mail: O.asghari@aut.ac.ir)
** Department of Mining and Metallurgy Engineering, Amirkabir University of Technology, Tehran, Iran. (E-mail: ardehez@aut.ac.ir).

At Sungun deposit, numerous cross-cutting quartz veinlets and micro-veinlets, developed in various stages of alteration and mineralization, provided suitable material for fluid inclusion investigations. Etminan (1977) was the first to recognize the presence of porphyry-type copper mineralization at Sungun through fluid inclusion studies. Based upon systematic sub-surface sampling, more detailed studies of fluid inclusions were carried out by Mehrpartou (1993) and Calagari (1997, 2004) and comprehensive micro thermometric data were accumulated. Additional fluid inclusion work on the Sungun PCD was presented by Hezarkhani and Williams-Jones (1998), Hezarkhani (2006).

In this research, it will be illustrated the differences between potassic and phyllic alterations based on fluid inclusion data. As expected, all variables such as homogenization temperature, salinity, pressure and density have higher average values in potassic than phyllic, but as will be described in this research, none of the parameters achieved from microthermometry of fluid inclusions, individually can lead to discriminate the potassic from the phyllic alteration.

GEOLOGICAL SETTING

The Sungun porphyry copper deposit is hosted by a diorite/granodiorite to monzonite/quartz-monzonite stock (Mehrpartou, 1993), located 75 km northwest of Ahar in the Azarbaijan province of northwest Iran (Figure 1). The stock is a part of the Sahand-Bazman igneous and metallogenic belt (northern Iran), a deeply eroded Tertiary volcanic field, roughly 100 by 1700 km in extent (from Turkey to Baluchistan in southern Iran), consisting mainly of rhyolite and andesite, with numerous felsic intrusions.

The Sungun porphyries intruded into Upper Cretaceous carbonate rocks, a series of Eocene arenaceous-argillaceous rocks, and a series of Oligocene dacitic breccias, tuffs and trachyandesitic lavas (Emami and Babakhani, 1991; Mehrpartou, 1993, Hezarkhani, 2006). The Sungun porphyries, which contain >500 Mt of sulfide reserves, grading 0.76 percent Cu and ~0.01 percent Mo, occur as stocks and dikes, and are series of calc-alkaline igneous rocks with a typical porphyritic texture (Hezarkhani and Williams-Jones 1998). They are situated at the northwestern part of a NW-SE trending Cenozoic magmatic belt (Sahand-Bazman) where the Sarcheshmeh PCD is also located. The Sungun stocks are divided into two groups: Porphyry Stock I is typically quartz monzodiorite where as Porphyry Stock II (which is investigated in this research) hosts the Sungun PCD and varies in composition from quartz monzonite through granodiorite to granite. Four series of cross-cutting dikes varying in composition from quartz monzodiorite to granodiorite, cut the Sungun stocks.

HYDROTHERMAL ALTERATION AND MINERALIZATION

Alteration assemblages and related mineralization in the Sungun porphyry copper deposit have been investigated by geological mapping and detailed mineralogical, petrographical and chemical studies of a large number of drill cores and outcrop samples from various parts of the stock (Figure 2). Hydrothermal alteration and mineralization at Sungun are centered on the stock and were broadly synchronous with its emplacement. Early hydrothermal alteration was dominantly potassic and propylitic, and was followed by later phyllic and argillic alteration.

Potassic alteration

The earliest alteration is represented by potassic mineral assemblages developed pervasively and as halos around veins in the deep and central parts of the Sungun stock (Hezarkhani et al. 1999). Potassic alteration is characterized by K feldspar. This alteration displays a close spatial association with mineralization, perhaps as much as 60 percent of the copper and all the molybde-

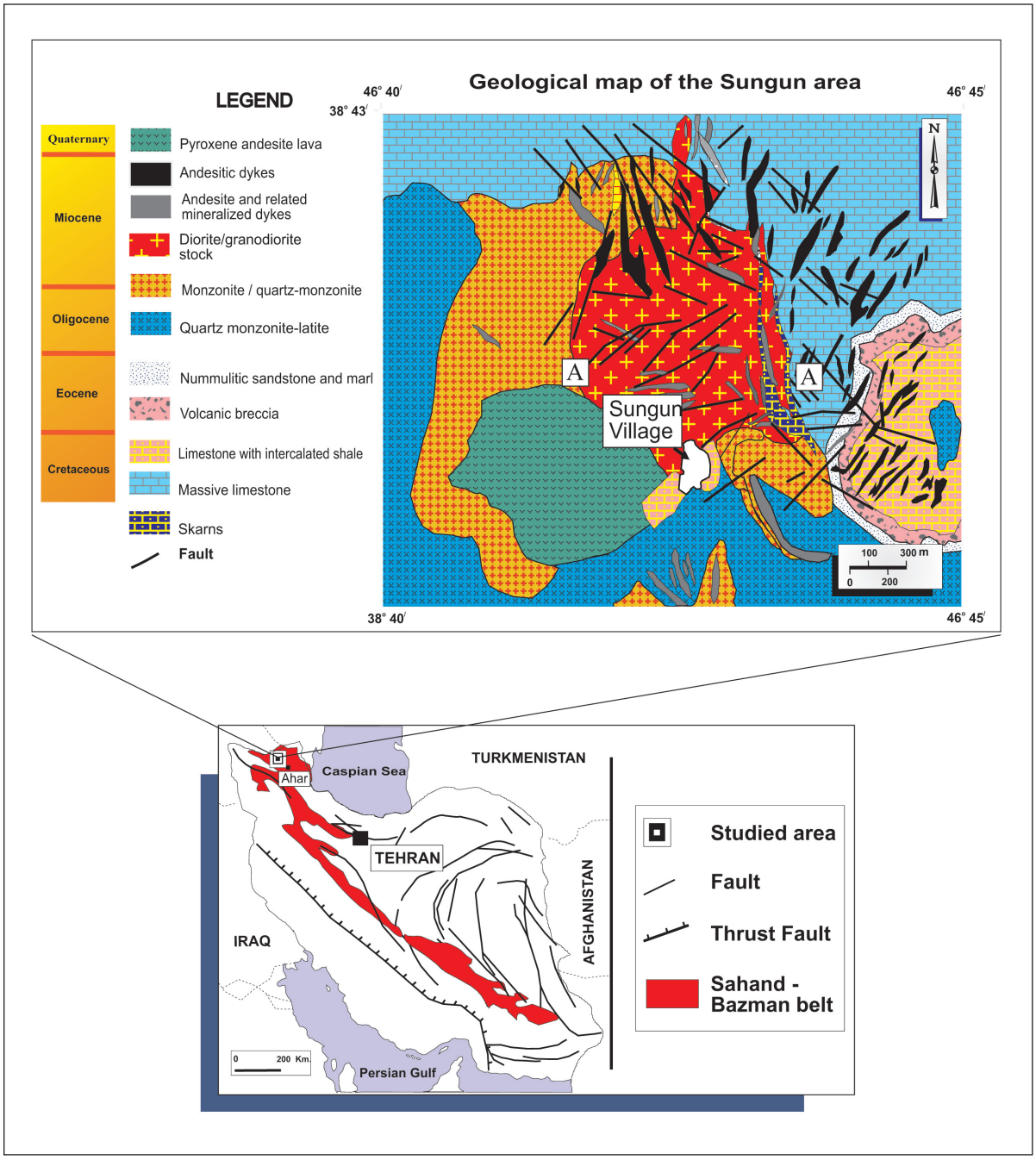

Figure 1- Below: Geological map of Iran showing Sahand-Bazman belt (modified from: Stocklin, 1976; Shahabpour, 2007); Above: Geological map of Sungun deposit area showing various types of intrusive rocks of dominantly Miosene ege and the outline of Cu-Mo porphyry type mineralizations. (Modified from Mehrparton, 1993 and Hezarkhani, 2006).

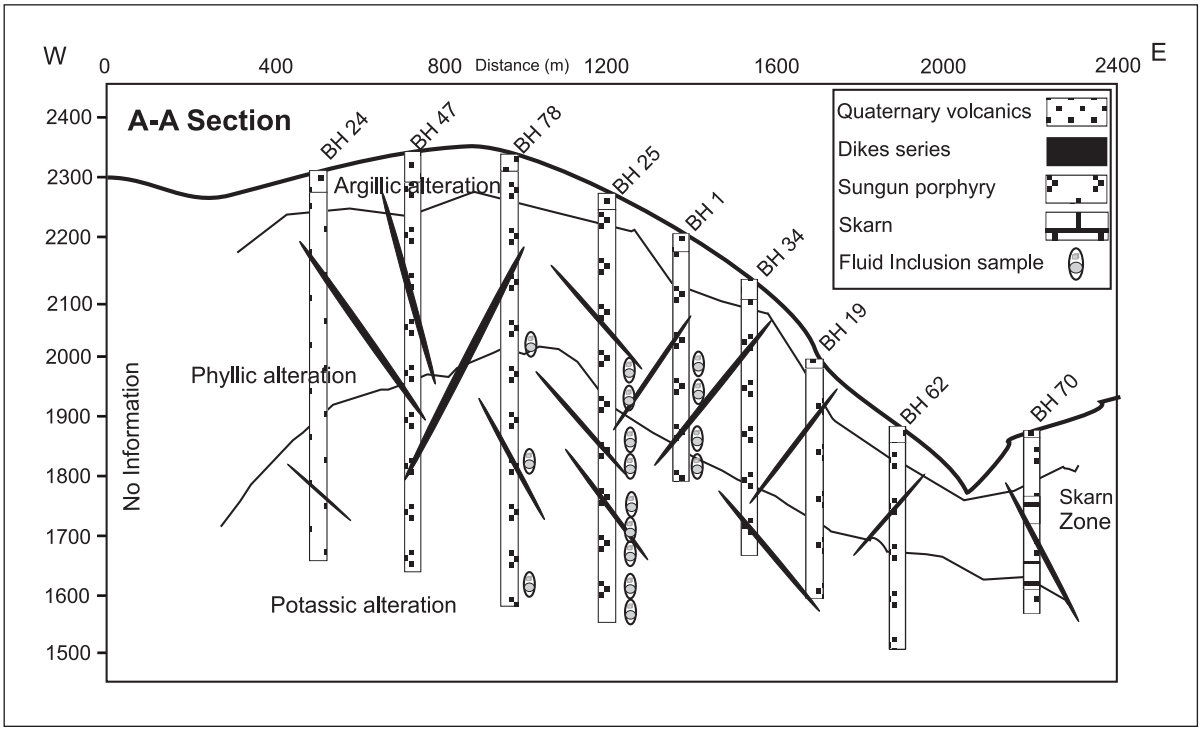

Figure 2- Profile along A-A in Figure 1 illustrating the position of diamond drill holes, dike series, and the pattern of hypogene alteration zones (potassici phyllic and argillic) in Porphyry Stock II.

num deposits were emplaced during this alteration episode (Hezarkhani and Williams-Jones 1998). On average, potassically altered rocks contain 28 percent plagioclase, 33 percent orthoclase, 20 percent quartz, 15 percent ferromagnesian minerals (mainly biotite, and sericite and chlorite after biotite) and 4 percent chalcopyrite, pyrite, zircon, scheelite, uraninite, bismuthinite, and rutile (Hezarkhani, 2006) (Figure 3a and plate 1a-1c).

Phyllic alteration

The change from transition alteration to phyllic alteration is gradual and is marked by an increase in the proportion of muscovite. Phyllic alteration is characterized by the replacement of almost all rock-forming silicates by sericite and quartz and overprints the earlier formed potassic and transition zones. Pyrite forms up to 5 vol. percent of the rock and occurs in veins and disseminations. Quartz veins are surrounded by weak sericitic halos (Plate 1d). Vein-hosted pyrite is partially replaced by chalcopyrite. Silicification was synchronous with phyllic alteration and variably affected a large part of the stock and most dikes. This observation is supported by whole-rock chemical analyses, which show that Si was added in, higher than for any other stage of the alteration (Hezarkhani and Williams-Jones 1998). In contrast to the transition zone, appreciable Cu was added to the rock during phyllic alteration. It is difficult to separate transition and phyllic alteration zones because of intense silicification during the latter alteration (Figure 3a).

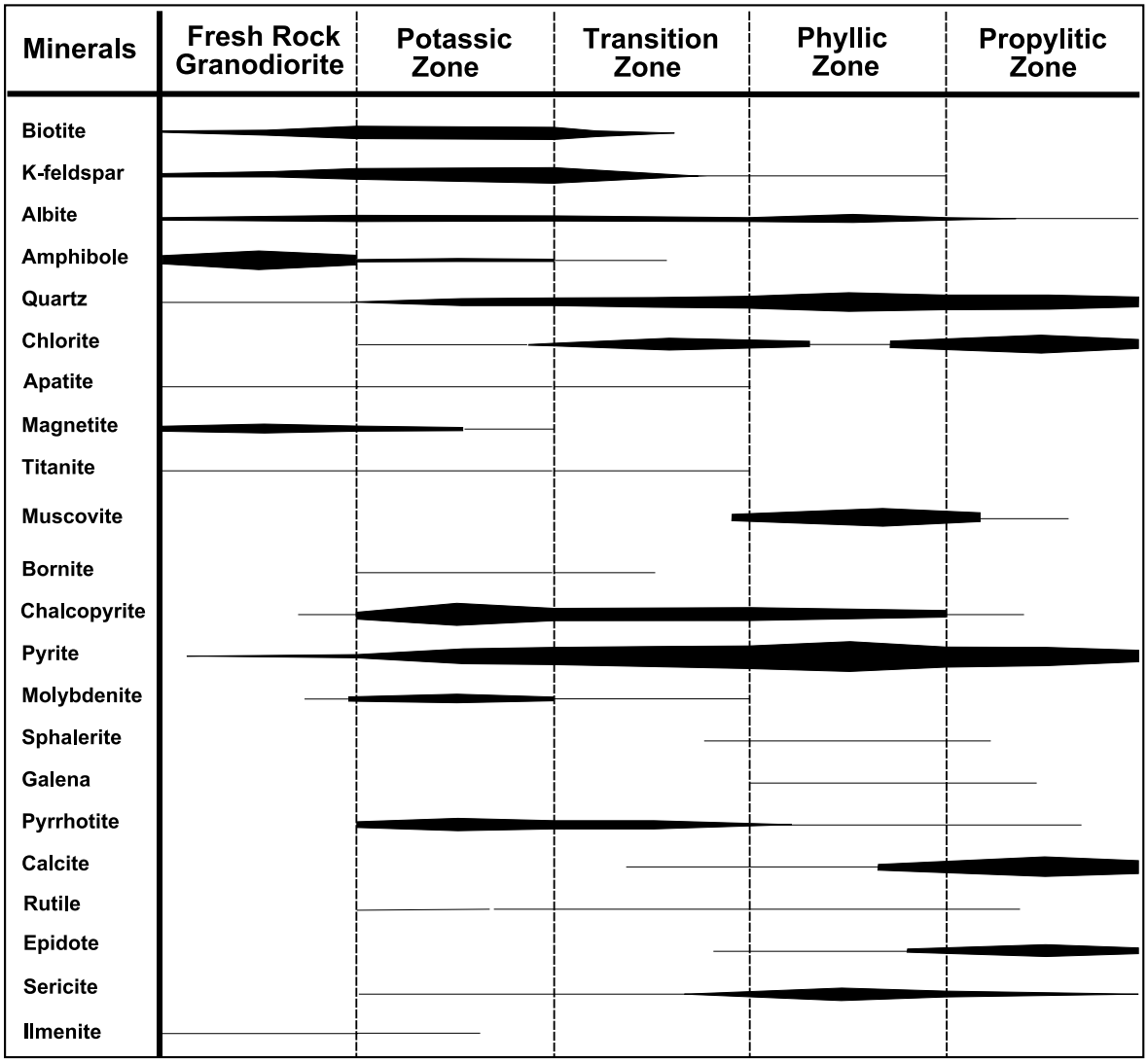

Figure 3a- Paragenetic sequence of the develpment of various alterations in porphyry stock II at Sungun. The thickness of the horizantal bars is related to the relative abundance of the mineral in the porphyry system (Hezarkhani and Williams-Jones, 1998; Calagari, 2004).

Mineralization

Hypogene copper mineralization was introduced during potassic and phyllic alteration, and exists as disseminations and veinlets form. During potassic alteration, the copper mineralization consisted of chalcopyrite and minor bornite; later hypogene copper mineralization consisted mainly of chalcopyrite (Plate 1e, 1f).

Alteration of feldspars and biotite (from potassically altered rocks) was accompanied by an increase in sulphide content outward from the central part of the stock. Copper mineralization

increases toward the margins of the central potassic zone, from less than 0.20 wt % to 0.85 wt%. There is also a positive correlation between silicification and copper mineralization. The maximum Cu grade is associated with biotite, orthoclase and sericite (potassic zone) while the pyrite content is highest (3-10 vol % of the rock) in the marginal quartz-sericite (phyllic) zone. The ratio of pyrite to chalcopyrite in the zone of richest hypogene copper mineralization seen in the potassic alteration zone is as low as 4:1, but toward the margins of the stock, the ratio increases to 15:1.

FLUID INCLUSIONS PETROGRAPHY

The Sungun deposit contains well-developed stockwork mineralization that is concentrated in the potassic and transition zones (the transition zone is actually the outermost part of the potassic zone and is characterized by a low content of biotite and abundant sericitization). Based on mineralogy and cross-cutting relationships, it is possible to distinguish four main groups of veins representing four episodes of vein formation: 1) quartz + molybdenite + anhydrite ± K-feldspar with sporadic pyrite, chalcopyrite and bornite, II) quartz + chalcopyrite + pyrite ± molybdenite, III) quartz + pyrite + calcite ± chalcopyrite + anhydrite (gypsum) + molybdenite, IV) quartz, and/or calcite, and/or gypsum ± pyrite (Figure 3b).

Fluid inclusions are abundant in quartz of all vein types, and range in diameter from 1µm up to 15 µm. The majority of inclusions examined during this study had diameters of 4 12 µm. Only fluid inclusions within the quartz crystals in quartz-sulfide and quartz-molybdenite veinlets were chosen for micro-thermometric analyses for two important reasons: (1) the inclusions are intimately associated with copper and molybdenum sulfides, (2) these veinlets contain inclusions >7µm which allows for more confident thermometric analysis. The individual quartz crystals contain numerous cross-cutting microfractures along which fluid inclusions are aligned (Plate 2a).

Since hydrothermal quartz, in the very early veins (Group I), was generally too fine grained to host fluid inclusions of sufficient size for study, most of the observations were restricted to fluid inclusions in coarse-grained quartz of early mineralized veins (Group II) and later quartz-anhydrite-pyrite veins (Group III). A preliminary classification of fluid inclusions was carried out based on the number, nature and relative proportions of phases at room temperature and led to recognition of the following types of fluid inclusions:

LV inclusions consist of liquid + vapor ± solid phases with the liquid phase volumetrically dominant. These fluid inclusions are common in all mineralized quartz veins and are abundant in Group II and III veins (Plate 2b). The diameters of these fluid inclusions ranges from 3 to 12 µm. LV inclusions are found in all vein groups, but occur in variable proportions. They are most abundant in the Group II and III veins, and rare in Group I veins. Most LV inclusions are distributed along healed fractures, and are of secondary origin.

VL inclusions are found in quartz phenocrysts from fresh rocks and in Group I, II and III quartz veins. Some of these inclusions occur in growth zones in Group I and II quartz veins, where they are accompanied by LVH fluid inclusions, indicating that most of them are primary. VL inclusions are generally elongated and have rounded ends, but some have negative crystal shapes. Some of the VL inclusions have variable liquid-vapor ratios, and may have formed from the necking down of LVH inclusions or heterogeneous entrapment of liquid and vapur.

LVH inclusions are found in all veins, from the deepest, potassically altered part of the stock

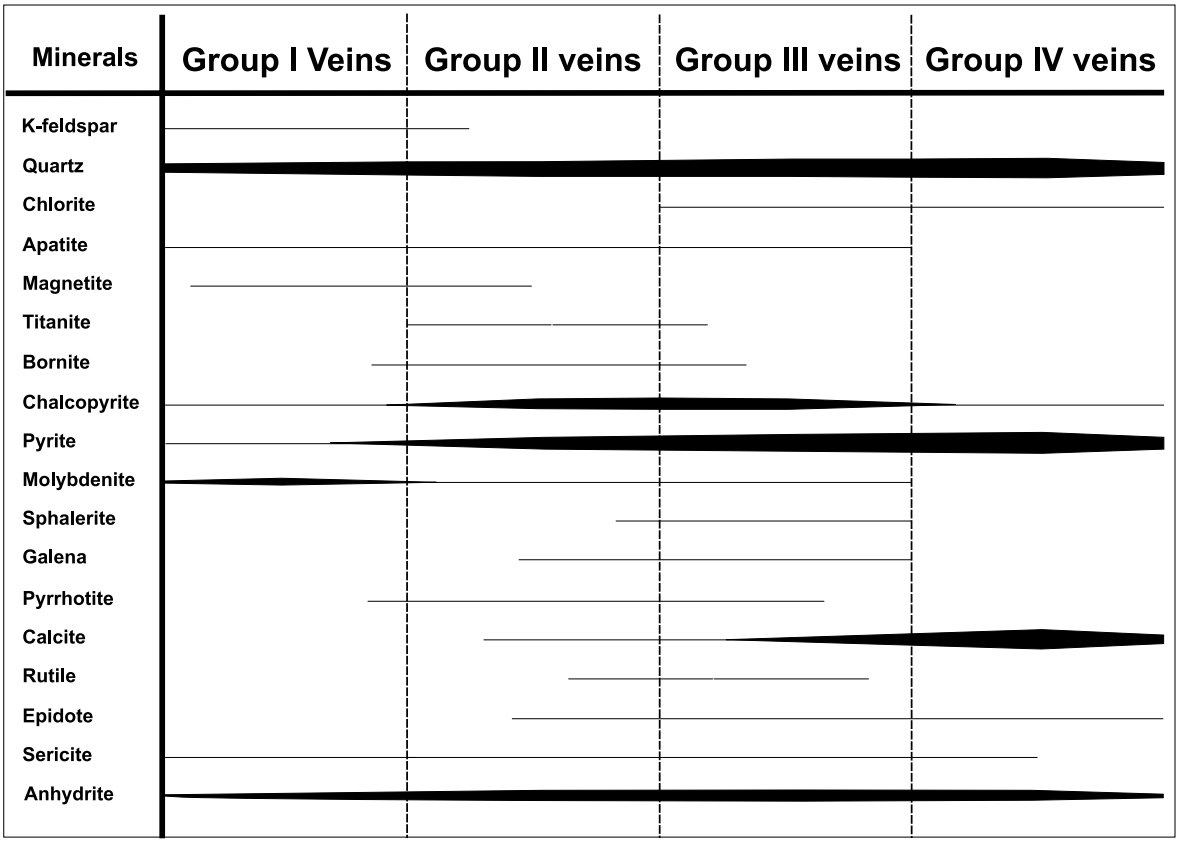

Figure 3b- Relative mineral abundances in various veins and veinlets in the Sungun deposit. Widths of bars denote qualitative abundances (Hezarkhani and Williams-Jones, 1998; Calagari, 2004).

through to the shallow level veins (Plate 2c, 2d). The fluids occupy cavities ranging from 1 μm to 15 μm in diameter. The coexistence of LVH inclusions and vapor-rich inclusions with consistent phase ratios in the growth zones of quartz grains, from potassic and phyllic alteration zones suggests a primary origin, and coexistence of two immiscible aqueous fluids.

The majority of LVH inclusions examined during this study had diameters of 4-12 μm. The 47 sub-surface samples containing quartz veinlets from diamond drill holes within the hypogene alteration zones in Porphyry Stock II, were selected for thermometric analyses.

FLUID INCLUSION INVESTIGATIONS

The samples were initially prepared for microscopic examination. Based on mineral content, the type of alteration is found and they are categorized as potassic and phyllic. The distribution pattern, shape, size, and phase content of fluid inclusions within the quartz crystals were examined applying a microscope (Table 1). Based upon their phase content, three types of inclusion are present at Sungun: (1) vapor-rich 2-phase, (2) liquid-rich 2-phase, and (3) multi-phase solid. Halite crystals are larger than the other solids and can be readily distinguished by their cubic shape. Similar characteristics are seen in fluid inclusion assemblages from other PCDs such as

Table 1- Statistical parameters of raw data based on fluid inclusion study and micro thermometry for 645 measurements in 47 samples totally and for high salinity inclusions (more than 27 wt% NaCl).

Type	Statistical	Salinity %	T_H	T_m	T_e (^oC)	Size(μm^2)	L/V
High and Low Salinity	Mean	23.9	355	-7.5	-38	22.4	2.9
	Standard	18.7	93	5.5	11.7	10.4	2.7
	Variance	348	8586	30.3	138	109	7.1
	Minumum	0.2	88	-33	-67	6	0.1
	Maximum	65.5	620	-0.5	-4	70	19
High and Low Salinity	Mean	43	375	-11.6	-46.9	24.5	3.4
	Standard	7.6	82	6.4	9.1	12.4	2.1
	Variance	57	6664	40.3	82.5	154	4.3
	Minumum	29	176	-33	-67.4	8	0.3
	Maximum	65.5	600	-1.2	-26	70	9

El Salvador, Chile (Gustafson and Hunt, 1975), Santa Rita, New Mexico (Ahmad and Rose, 1980), Bingham, Utah (Roedder, 1971), Yandera and Panguna, Papua New Guinea (Watmuff, 1978; Eastoe, 1978), Copper Canyon, Nevada (Nash, 1976), Bajo de la Alumbrera and Argentina (Ulrich et al., 2001).

a- Micro-thermometric analysis

The Linkam operating unit was applied to measure the temperatures of phase changes in fluid inclusions, which operates by passing pre-heated or pre-cooled N_2 gas around the sample (Werre et al., 1979). Stage calibration was performed using synthetic and/or well-known fluid inclusions. Accuracy at the standard reference temperatures was ±0.2°C at -56.6°C (triple point of CO_2), ±0.1°C at 0°C (melting point of ice), ±2°C at 374.1°C (critical homogenization of H_2O), and ±9°C at 573°C (alpha to beta quartz transition). The heating rate was approximately 1°C/min near the temperatures of phase transitions. Thermometric analyses were performed principally on fluid inclusions which were relatively large (>7 μm). Freezing and heating experiments helped to determine the approximate salinity (wt% NaCl equivalent) and homogenization temperature (T_h); respectively (Table 1). The heating stage was used for all types of inclusion. For non-halite bearing inclusions the homogenization temperature of liquid and vapor (either L+V → L or L+V → V) was recorded. In the halite-bearing inclusions, two points: (1) $T_{s(NaCl)}$ (the temperature at which halite dissolves) and (2) $T_{h(L-V)}$ (temperature of vapor and liquid homogenization) were recorded.

b- Homogenization temperatures

The temperatures of initial (T_e) and final melting of ice ($T_{m\ ice}$) were measured on types LV, VL,

and LVH fluid inclusions. The temperature of initial ice melting (T_e) of most LV fluid inclusions were between -23° and -24°C, suggesting that NaCl is the principal salts in solution. The T_e value of VL fluid inclusions ranges from - 20° to -46°C with a mode of ~-22°C, suggesting that Na and K are the dominant cations in the solution, but there may be other components for example Mg and Ca which could not be measurable by this method. The low T_e (-31°C to -46°C) for some of the VL inclusions could indicate that these inclusions are the products of necking down of LVH inclusions.

The eutectic temperatures that could be measured in LVH inclusions range from -30° to -64°C, suggesting important concentrations of Fe, Mg, Ca, and/or other components in addition to Na and K in this type of inclusion. The $T_{m\ ice}$ values for LV inclusions range from -5° to -8°C, corresponding to salinities of 5.7 wt% NaCl equivalent respectively (Sterner et al., 1988). The $T_{m\ ice}$ value for VL inclusions varies from -0.4°C to -12°C, which corresponds to a salinity of between 0.8 and 12.2 wt% NaCl equivalent.

LV fluid inclusions homogenize to liquid T_h (L+V → L) at temperatures between 523° and 298°C. Most of VL inclusions homogenize to vapor T_h (V+L → V) between 351° and 600 (°C). The frequency distribution of halite-bearing inclusions homogenizing by halite disappearance ($T_{s(NaCl)} > T_{H(L-V)}$) display a wide range of $T_{s(NaCl)}$ values, varying from 220 to 583 (°C). Salinities based on the halite dissolution tempe-rature range from 29.7 to 61.1 wt % NaCl equivalent (Table 2).

The halite-bearing inclusions homogenizing by simultaneous disappearance of halite vapor and/or by vapor disappearance ($T_{s(NaCl)} \leq T_{H(L-V)}$) show a similar range of distribution and their $T_{H(L-V)}$ values vary from 200 to 580 (°C). Some LVH inclusions homogenized by vapor disappearance and by contrast, some LVH inclusions homogenized mainly by halite dissolution. Anhydrite and chalcopyrite did not dissolve on heating to temperatures in excess of 600°C. Chalcopyrite was identified on the basis of its optical characteristics (opacity and triangular cross section) and composition in opened inclusions (SEM-EDAX analyses yielded peaks for Cu, Fe and S). Anhydrite forms transparent anisotropic prisms and was shown by SEM-EDAX analyses to consist only of Ca and S (elements lighter than F could not be analyzed) (Hezarkhani and Williams-jones, 1998).

Table 2- Descriptive statistics of primary inclusion's data for high salinity inclusions (more than 27 wt% NaCl).

Statistical parameter	Salinity	T_h	T_m	T_e	Size(μm^2)	L/V Ratio
Mean	43	375	-11.6	-46.9	24.5	3.4
Standard Deviation	7.6	82	6.4	9.1	12.4	2.1
Sample Variance	57	6664	40.3	82.5	154	4.3
Minimum	29.7	220	-33	-67.4	8	0.3
Maximum	61.1	583	-1.2	-26	70	9

c- Salinity of the inclusion fluids

Halite-bearing and non-halite-bearing liquid-rich inclusions at Sungun, exhibit a wide variation in salinity, ranging from 0.2 to 65.5 wt% (Figure 4). There are many halite-bearing fluid inclusions which have $T_{s(NaCl)} > T_{H(L-V)}$ and the discrepancy between $T_{s(NaCl)}$ and $T_{H(L-V)}$ in some inclusions may reach ~98 °C (Figure 5). These inclusions may suggest entrapment of supersaturated (with respect to NaCl) fluid or high pressure conditions of entrapment (Table 3, No. 12). However, there are still many halite-bearing inclusions whose data points lie around and below the halite saturation curve ($T_{s(NaCl)} < T_{H(L-V)}$) (Figure 5) which, in turn, denotes trapping of saturated and under saturated fluids, respectively.

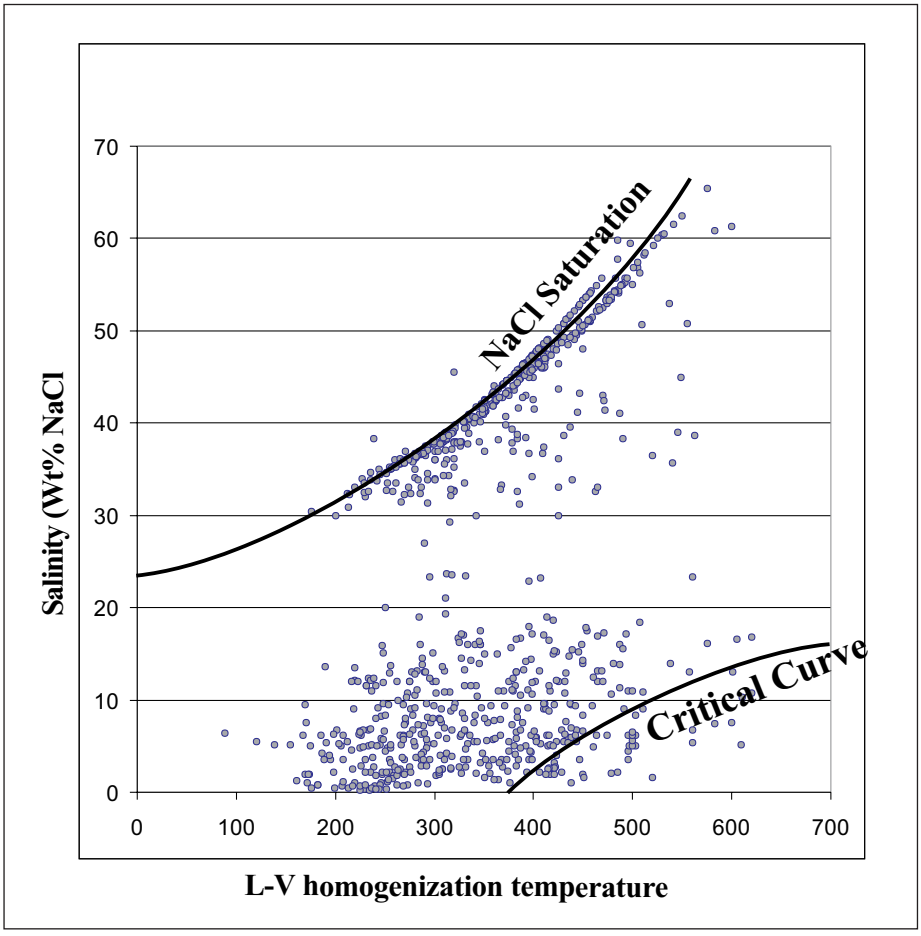

Figure 4- Salinity versus $T_{H(L-V)}$ illustrating the distribution pattern of the data points relative to the NaCl saturation and critical curves (NaCl saturation and critical curves from Cloke and Kesler, 1979). Dashed lines referring to vapor of NaCl solutions at the indicated temperatures and salinity (from Roedder, 1984).

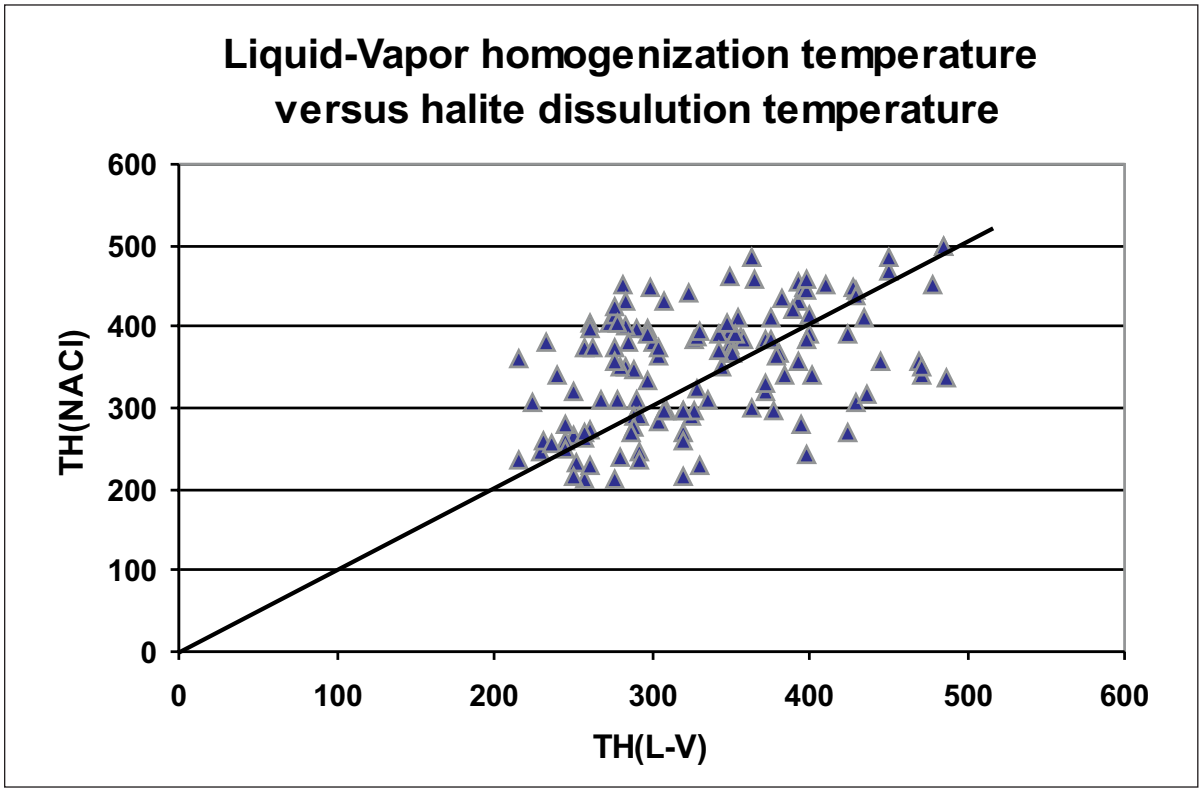

Figure 5- Liquid-vapor homogenization temperature ($T_{H(L-V)}$) versus halite dissolution temperature ($T_{H(NaCl)}$) for halite - bearing inclusions at Sungun (the diagonal line ($T_{H(L-V)} = T_{S(NACl)}$) from Shepherd et al., 1985). For calculating the pressure we used points over the diagonal line, where $T_{S(NACl)}>T_{H(L-V)}$.

Based on the Brown and Lamb (1989) is method, to measure the geological pressure the applied fluid inclusions must be halite-and gas-bearing with high salinity ones, which is why that these type of fluid inclusions are used from now on. Table 2 shows the statistical properties of the fluid inclusions with the salinities more than 27 wt% equivalent.

The point pressure and hydrothermal fluid density in the NaCl-H_2O system is calculated for 47 samples with using 3 parameters including Th → Halite (°C), Th → Vapor (°C) and salinity (wt% NaCl), based on Brown and Lamb (1989) is equation by the Flincor software (Brown, 1989). Fluid pressures varies from 261 to 2148 bars (Table 3)

COMPARING THE RESULTS IN TWO ALTERATIONS

As discussed earlier, the analyses were done on the three-phase fluid inclusions that were in the quartz veins adjacent to the mineralization (in different alterations). As we expected, this fluid inclusions shows high salinity. With the investigation of the table 4 it could be seen that the average salinity in potassic alteration is a little bit higher than the average salinity of the phyllic alteration, but they are very close to each other, as mentioned in Hezarkhani and Williams-Jones (1998).

The results show that the average of Th, salinity, pressure and density of fluids in quartz

Table 3- Achieved data from 47 locations in 13 boreholes separated into potassic and phyllic. Based on microscopic studies and XRF analysis 22 of them defined as potassic and 25 of them defined as phyllic alteration.

No.	BH No.	Alteration	Elevation (m)	Cu (%)	Th→H (^{o}C)	Salinity (%)	Th→V (^{o}C)	Pressure (bar)	Density (gr/cm^{3})
1	BH	PHY	1848	0.73	337	39.8	297	836	1.11
2	BH	PHY	1808	0.86	351	42.5	319	770	1.15
3	BH	POT	1801	0.68	394	46.5	368	711	1.12
4	BH	POT	1774	0.64	371	44.8	350	583	1.11
5	BH	POT	1660	0.3	373	45.1	321	1165	1.14
6	BH	POT	1615	0.75	398	47.2	311	1981	1.19
7	BH	POT	1603	0.63	358	43.1	277	1688	1.16
8	BH	POT	1594	0.98	337	41.6	288	1030	1.14
9	BH	POT	1581	0.65	347	42.6	321	619	1.12
10	BH	PHY	1622	0.49	460	54.6	451	654	1.13
11	BH	POT	1592	0.7	359	43.3	298	1406	1.19
12	BH	POT	1729	0.29	398	45.5	300	2108	1.17
13	BH 1	PHY	1853	0.6	410	46	395	560	1.08
14	BH 1	PHY	1847	0.52	450	48	427	838	1.07
15	BH 1	PHY	1843	0.31	430	47.8	411	713	1.08
16	BH 1	PHY	1830	0.48	312	36	298	324	1.07
17	BH 1	PHY	1827	0.64	234	33.5	212	446	1.13
18	BH 1	PHY	1826	0.64	220	33	200	410	1.13
19	BH 1	PHY	1824	0.85	250	34	225	502	1.12
20	BH 2	PHY	1876	1.06	350	37	343	261	1.04
21	BH 2	PHY	1861	0.85	355	38	344	334	1.04
22	BH 2	PHY	1823	0.57	414	46.9	384	854	1.1
23	BH 2	PHY	1821	0.71	410	48	400	485	1.1
24	BH 2	PHY	1818	1.21	423	49	408	602	1.1
25	BH 2	PHY	1813	1.17	380	36	349	655	1.02
26	BH 2	PHY	1746	0.85	399	36	393	342	0.97
27	BH 2	PHY	1741	0.9	428	46	414	590	1.06
28	BH 3	PHY	1807	0.52	382	38.3	337	913	1.05
29	BH 3	PHY	1801	0.53	425	46.4	407	664	1.07
30	BH 4	POT	1707	0.1	356	42	331	599	1.1
31	BH 5	PHY	1711	0.12	404	46	390	528	1.08
32	BH 6	POT	1647	0.72	385	45.5	381	303	1.09
33	BH	POT	2080	0.41	461	52.7	424	1257	1.13
34	BH	POT	1813	1.31	431	47.7	398	965	1.09
35	BH	POT	1661	0.63	444	49.9	403	1210	1.12
36	BH	POT	1780	0.42	442	49.7	410	1020	1.11
37	BH	POT	1543	0.23	455	51.1	403	1483	1.13
38	BH	PHY	1671	0.76	404	45.4	388	557	1.08
39	BH	POT	1792	0.61	418	47.3	355	1503	1.13
40	BH	POT	1685	0.65	583	60.9	550	2148	1.13
41	BH	POT	1673	0.32	475	53.6	432	1452	1.13
42	BH	POT	1659	0.4	406	46.7	362	1098	1.12
43	BH	PHY	1959	0.66	394	45.2	358	875	1.11
44	BH	PHY	1918	0.47	389	44.5	335	1214	1.12
45	BH	PHY	1783	0.55	388	43.8	363	646	1.09
46	BH	POT	1676	0.42	462	32.6	408	998	1.14
47	BH	POT	1631	0.79	447	38.5	404	962	0.99

Table 4- Descriptive statistics of 25 samples from phyllic alteration and 22 samples from potassic alteration.

	Descriptive	Elevation (m)	Cu (%)	Th→H (^oC)	Salinity (%NaCl)	Th→V (^oC)	Pressure (bar)	Density (gr/cm^3)
Potassic	Mean	1695	0.57	414	46.3	368	1195	1.12
	S.D.	116	0.27	56	5.7	63	498	0.04
	Var.	13351	0.07	3181	32.7	3925	247652	0.002
	Min	1543	0.10	337	32.6	277	303	0.98
	Max	2080	1.31	583	60.9	583	2148	1.19
Phyllic	Mean	1811	0.68	376	42.5	354	623	1.08
	S.D.	71	0.25	64	5.8	66	222	0.04
	Var.	5092	0.06	4039	34	4374	49497	0.002
	Min	1622	0.12	220	33	200	261	0.97
	Max	1959	1.21	460	54.6	451	1214	1.15
Total	Mean	1757	0.63	394	44.2	360.	891	1.1

veinlets of potassic alteration are more than the ones in phyllically altered samples.

- In potassic alteration, the average homogenization temperature is 413.6 °C while in phyllic alteration it is 375.9 °C. As it is expected in potassic alteration, the temperature of hydrothermal is higher than the phyllic one, but there is not much difference between them.

- The salinity of the hydrothermal fluid has a high coherency with homogenization temperature, so the average amount of salinity in potassic samples is 46.3 (wt% NaCl) which is a little bit higher than that of the phyllic samples (42.5 wt% NaCl). As discussed above, the analyses were done on the three-phase fluid inclusions and as expected, this type of fluid inclusion shows high salinity in both alterations.

- Based on the location of potassic alteration, which is located beneath the phyllic alteration, we expect the lithostatic pressure is much more than the phyllic one, so it is realized that the average pressure in the potassic alteration is 1195 (bar) while the pressure average in phyllic is about 623 (bar).

- The density depends on the amount of the salinity of hydrothermal fluid, so the average density of the samples in potassic alteration is 1.124 (gr/cm^3) which is higher than the phyllic one (1.083 gr/cm^3).

CONCLUSIONS

Based on various comprehensive studies on Sungun Copper deposit, it is illustrated that the Sungun deposit is a porphyry system and the potassic and phyllic alterations contain copper

sulfide minerals extensively. The primary multiphase inclusions within the quartz crystals in quartz-sulfide and quartz-molybdenite veinlets (quartz associated with sulfide minerals) were chosen for micro-thermometric analyses and considered to calculate the geological pressure and hydrothermal fluid density.

Early hydrothermal alteration produced a potassic assemblage (orthoclase-biotite) in the central part of the Sungun stock. Propylitic alteration occurred contemporaneously with potassic alteration. But in the peripheral parts of the stock, phyllic alteration occurred later, overprinting these earlier alterations. Based on fluid inclusion studies in the Sungun deposit, potassic alteration and associated Cu mineralization were caused by a high temperature and high salinity fluid of dominantly magmatic origin. The early hydrothermal fluids are represented by high temperature (337 °C to 583 °C), high salinity (up to 60 wt % NaCl equiv.) liquid-rich fluid inclusions, and high temperature (320 °C to 550 °C), low-salinity, vapor-rich inclusions. Phyllic alteration and copper leaching resulted from the inflow of oxidized and acidic meteoric waters with decreasing temperature (ranging from 220-460 °C, with a mean of 376 °C) of the system.

The average of all four measured variables (homogenization temperature, salinity, pressure and density) is higher in potassic samples than phyllic ones, but it is not possible to draw a vertical line and separate the two alteration samples. It means the thermodynamic conditions for those alterations are close together and other parameters could affect the mineral precipitation and mineral assemblages in the alteration zones.

Manuscript received March 3, 2008

REFERENCES

Ahmad, S.N., and Rose, A.W., 1980. Fluid inclusions in porphyry and skarn ore at Santa Rita, New Mexico. Economic Geology 75, 229-250.

Beane, R. E. and Titley, S.R., 1981. Porphyry copper deposits: Part II. Hydrothermal alteration and mineralization: Economic Geology 75th Anniversary Volume, 235-269.

_____ and Bodnar, R.J., 1995. Hydrothermal fluids and hydrothermal alteration in porphyry copper deposits. In: Wahl, P.W., Bolm, J.G. (Eds.), Porphyry Copper Deposits of the American Cordillera, Tucson, Arizona, Arizona Geological Society, Arizona, 83-93.

Brown, P. E., 1989. FLINCOR: a microcomputer program for the reduction and investigation of fluid inclusion data. American Mineralogist, 74, 1390-1393.

_____ and Lamb, W.M., 1989. P- V-T properties of fluids in the system H_2O-CO,-NaCI: New graphical presentations and implications for fluid inclusion studies. Geochimica et Cosmochimica Acta, 53, 1209-1221.

Burnham, C. W., 1979. Magmas and hydrothermal fluids. In: H. L. Barnes (ed), Geochemistry of Hydrothermal ore deposits, John Wiley & Sons, 71-136.

Calagari, A. A., 1997. Geochemical, stable isotope, noble gas, and fluid inclusion studies of mineralization and alteration at Sungun porphyry copper deposit, East Azarbaidjan, Iran: Implication for genesis. Unpublished PhD Thesis. Manchester University, Manchester, 537 p.

Calagari, A. A., 2004. Fluid inclusion studies in quartz veinlets in the porphyry copper deposit at Sungun, East-Azarbaidjan, Iran, Journal of Asian Earth Sciences 23, 179-189.

Chivas, A.R. and Wilkins, R.W.T., 1977. Fluid inclusion studies in relation to hydrothermal alteration and mineralization at the Koloula porphyry copper prospect, Guadalcanal. Economic Geology, 7,153-169.

Cloke, P.L. and Kesler, S.E., 1979. The halite trend in hydrothermal solutions. Economic Geology 74, 1823-1831.

Dilles, J.H. and Einaudi, M.T., 1992. Wall-rock alteration and hydrothermal flow paths about the Ann-Mason porphyry copper deposits, Nevada-a 6-km vertical reconstruction. Economic Geology, 87, 1963-2001.

Eastoe, C. G., 1978. A fluid inclusion study of the Panguna porphyry copper deposit, Bougainville, Papua New Guinea: Economic Geology, 73, 721 748.

Emami, M.H., and Babakhani, A.R., 1991. Studies of geology, petrology, and litho-geochemistry of Sungun Cu-Mo deposit, Iranian Ministry of Mines and Metals, 61.

Etminan, H., 1977. The discovery of porphyry copper-molybdenum mineralization adjacent to Sungun village in the northwest of Ahar and a proposed program for its detailed exploration. Confidential Report, Geological Report, Geological Survey of Iran, 26 p.

Gustafson, L. B., and Hunt, J. P., 1975. The porphyry copper deposit at El Salvador, Chile: Economic Geology, 70, 857 912.

Hedenquist, J.W. and Richards, J.P., 1998. the influence of geochemical techniques on the development of genetic models for porphyry copper deposits. In: Richards JP, Larson PB (eds) Techniques in hydrothermal ore deposits geology. Rev Economic Geology 10, 235-256.

Heinrich, C.A., 2005. The physical and chemical evolution of low-salinity magmatic fluids at the porphyry to epithermal transition: a thermodynamic study Mineralium Deposita, 39, 864-889.

_____, Pettke, T., Halter, W.E., Aigner-Torres, M., Audetat, A., Gunther, D., Hattendorf, B., Bleiner, D., Guillong, M. and Horn, I., 2003. Quantitative multi-element analysis of minerals, fluid and melt inclusions by laser-ablation inductively-coupled-plasma mass-spectrometry. Geochimica et Cosmochimica Acta, 67, 3473-3497

Hezarkhani, A., 2006, Petrology of Intrusive rocks within the Sungun Porphyry Copper Deposit, Azarbaijan, Iran. Journal of Asian Earth Sciences. 73, 326-340.

_____ and Williams-Jones, A.E., 1998. Controls of alteration and mineralization in the Sungun porphyry copper deposit, Iran: Evidence from fluid inclusions and stable isotopes. Economic Geology, 93, 651-670.

_____ Williams-Jones, A. E. and Gammons, C. H., 1999. Factors controlling copper solubility and chalcopyrite deposition in the Sungun porphyry copper deposit, Iran, Mineralium Deposita, 34, 770-783.

Kehayov, R., Bogdanov, K., Fanger, L., von Quadt. A., Pettke, T. and Heinrich, C.A., 2003. The fluid chemical evolution of the Elatiste porphyry Cu-Au-PGE deposit, Bulgaria. In: Eliopoulos DG (ed) Mineral exploration and sustainable development. Millpress, Rotterdam, 1173-1176.

Mehrpartou, M., 1993. Contributions to the geology, geochemistry, Ore genesis and fluid inclusion investigations on Sungun Cu-Mo porphyry deposit, northwest of Iran. Unpublished PhD Thesis. University of Hamburg, Germany, 245 p.

Nash, J. T., 1976. Fluid inclusion petrology data from porphyry copper deposits and applications to exploration: U.S. Geological Survey Proffessional Paper, 907 D, 16p.

Quan, R.A., Cloke, P.L., and Kesler, S.E., 1987. Chemical analyses of halite trend inclusions from the Granisle porphyry copper deposit, British Columbia. Economic Geology, 82, 1912-1930.

Redmond, P.B., Einaudi, M.T., Inan, E.E., Landtwing, M.R. and Heinrich, C.A., 2004. Copper deposi-

tion by fluid cooling in intrusioncentered systems: new insights from the Bingham porphyry ore deposit, Utah. Geology 32(3), 217-220.

Roedder, E., 1971. Fluid inclusion studies on the porphyry copper-type ore deposits at Bingham (Utah), Butte (Montana), and Climax (Colorado). Economic Geology, 66, 98-120.

_____, 1984. Fluid inclusions, Reviews in Mineralogy, vol. 12. Book Crafters, Inc, Michigan, 644 p.

_____ and Bodnar, R.J., 1980. Geologic pressure determination from fluid inclusion studies. Annual Review of Earth and Planetary Science 8, 263-301.

_____, 1984. Fluid inclusions: Reviews in mineralogy, Ribbe, P. H. (ed), 12, 644 p.

Shepherd, T., Rankin, A.H., and Alderton, D.H.M., 1985. A Practical Guide to Fluid Inclusion Studies, Blackie, London, 239 p.

Sillitoe, R.H. and Hedenquist, J.W., 2003. Linkages between volcanotectonic settings, ore-fluid compositions and epithermal precious metal deposits. In: Simmons SF, Graham I (eds) Volcanic, geothermal and ore-forming fluids: rulers and witnesses of processes within the earth. Economic Geology Special Publucation, 343 p.

Sillitoe, R.H., 1997. Characteristics and controls of the largest porphyry copper-gold and epithermal gold deposits in the circum- Pacific region. Australian Journal of Earth Sciences, 44(3), 373-388.

Sourirajan, S., and Kennedy, G.C., 1962. The system H_2O-NaCl at elevated temperatures and pressures. American Journal of Science, 260, 115-141.

Sterner, S. M., Hall, D. L., and Bodnar, R. J., 1988. Synthetic fluid inclusions. V. Solubility of the system NaCl-KCl-H_2O under vapor-saturated conditions. Geochimica et Cosmochimica Acta, 52, 989- 1005.

Stocklin, J.O., 1977. Structural correlation of the Alpine ranges between Iran and Central Asia. Mem. H. Aser. Geological Society of France, 333-353.

Tosdal R.M. and J.P. Richards., 2001. Magmatic and structural controls on the development of porphyry Cu±Mo±Au deposits. In: Richards, J.P. and Tosdal, R.M. (eds), Structural controls on ore genesis. Reviews in Economic Geology, 157-180

Ulrich, T., Gunther, D., and Heinrich, C.A., 2001. The evolution of a porphyry Cu-Au deposit, based on La-ICP-MS analysis of fluid inclusions, Bajo de la Alumbrera, Argentina. Economic Geology 96, 1743-1774.

Urusova, M.A., 1975. Volume properties of aqueous solutions of sodium chloride at elevated temperatures and pressures. Russian Journal of Inorganic Chemistry 20, 1717-1721.

Watmuff, G., 1978. Geology and alteration-mineralization zoning in the central portion of the Yandera porphyry copper prospect, Papua New Guinea. Economic Geology 73, 829-856.

PLATES

PLATE I

Figure a- Scanning electron photomicrographs: Molybdenite with associated anhedral bismuthinite and pyrite.

Figure b- Quartz associated with pyrite altered to chalcopyrite. All fluid inclusions have been measured from quartz veins associated with ore minerals.

Figure c- Plagioclase and calcite veins in potassically altered sample from BH104-351m (optical microscope, crossed polars).

Figure d- Quartz veins are surrounded by weak sericitic halos in phyllically altered samples from BH2-145m.

Figure e and f copper mineralization in chalcopyrite from potassic and phyllic samples.

Abbreviations: Bi= bismuthinite, Cp=chalcopyrite, Mo=molybdenite, Py=pyrite, Qtz=quartz.

PLATE - I

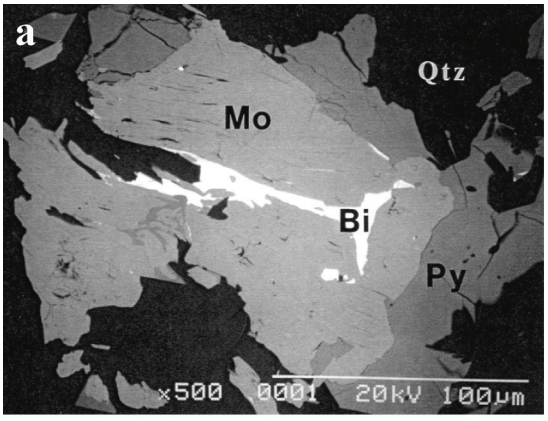
a
Qtz
Mo
Bi
Py
×500 0001 20kV 100µm

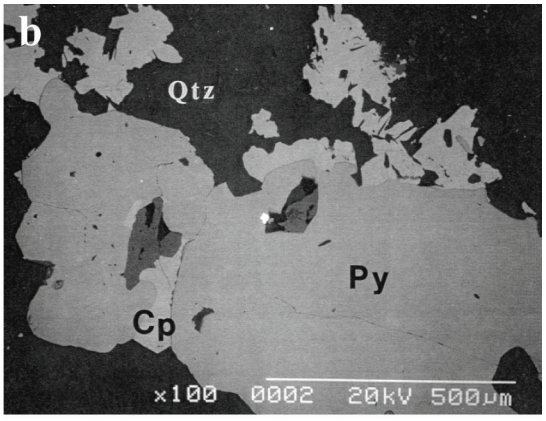
b
Qtz
Py
Cp
×100 0002 20kV 500µm

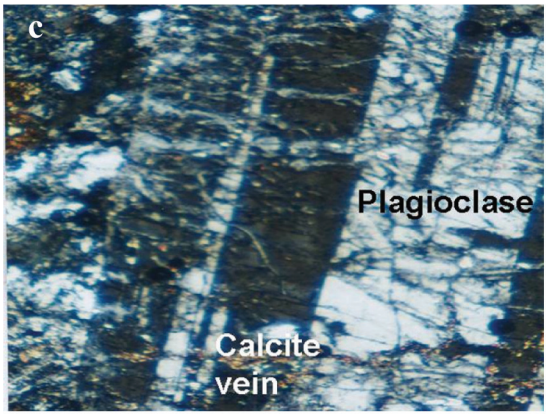
c
Plagioclase
Calcite
vein

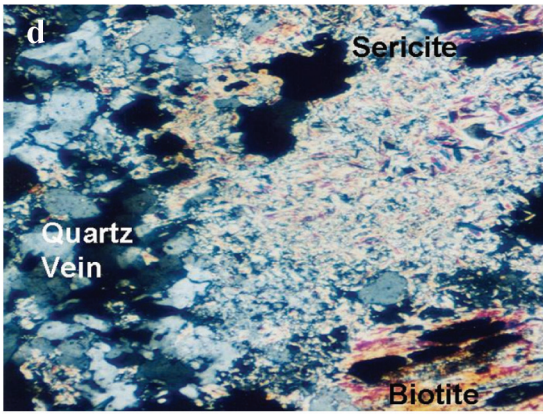
d
Sericite
Quartz
Vein
Biotite

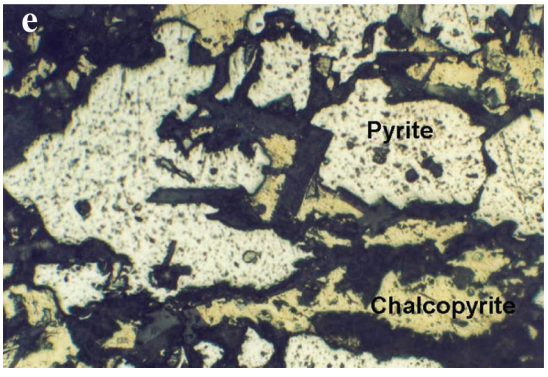
e
Pyrite
Chalcopyrite

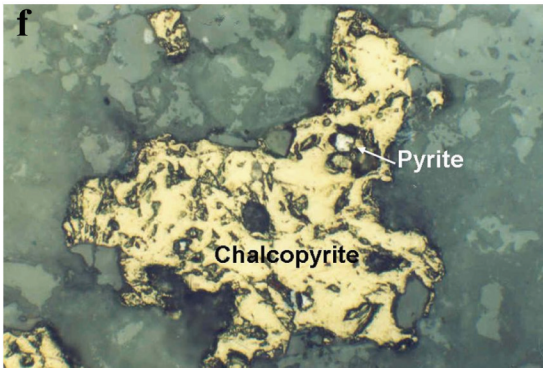
f
Pyrite
Chalcopyrite

PLATE II

Photomicrographs of different inclusion types within mineralized quartz vein from Sungun.

Figure a- Secondary fluid inclusions;

Figure b- Secondary biphase (VL and LV) inclusions,

Figure c- primary polyphase inclusion from potassic alteration assemblage (sample no. 42) and

Figure d- primary inclusion from Phyllic alteration assemblage (sample no.18).

All photographs were taken at ambient laboratory temperature. See text for discussion.

PLATE - II

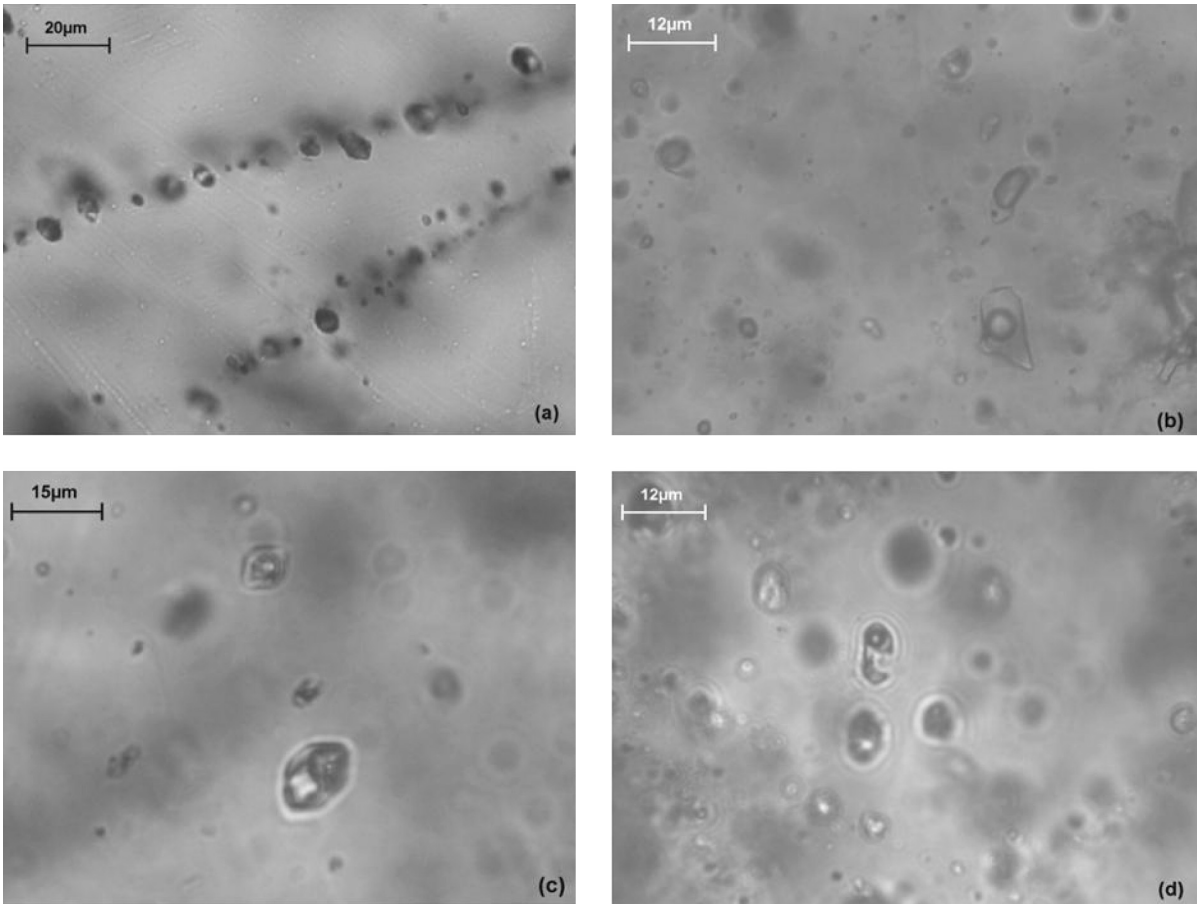

BOS SAYFA